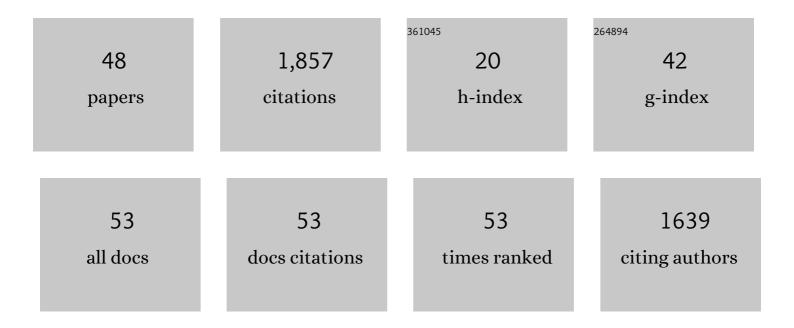
Arnaud Mazurier

List of Publications by Year in descending order

Source: https://exaly.com/author-pdf/8088004/publications.pdf Version: 2024-02-01



#	Article	IF	CITATIONS
1	How Neanderthal molar teeth grew. Nature, 2006, 444, 748-751.	13.7	276
2	Large colonial organisms with coordinated growth in oxygenated environments 2.1 Gyr ago. Nature, 2010, 466, 100-104.	13.7	235
3	A new Late Miocene great ape from Kenya and its implications for the origins of African great apes and humans. Proceedings of the National Academy of Sciences of the United States of America, 2007, 104, 19220-19225.	3.3	167
4	Dental tissue proportions and enamel thickness in Neandertal and modern human molars. Journal of Human Evolution, 2008, 55, 12-23.	1.3	148
5	Dental maturational sequence and dental tissue proportions in the early Upper Paleolithic child from Abrigo do Lagar Velho, Portugal. Proceedings of the National Academy of Sciences of the United States of America, 2010, 107, 1338-1342.	3.3	78
6	Dental developmental pattern of the Neanderthal child from Roc de Marsal: a high-resolution 3D analysis. Journal of Human Evolution, 2009, 56, 66-75.	1.3	66
7	Endostructural characterization of the H.Âheidelbergensis dental remains from the early Middle Pleistocene site of Tighenif, Algeria. Comptes Rendus - Palevol, 2013, 12, 293-304.	0.1	57
8	Technical note: Morphometric maps of long bone shafts and dental roots for imaging topographic thickness variation. American Journal of Physical Anthropology, 2010, 142, 328-334.	2.1	56
9	The 2.1 Ga Old Francevillian Biota: Biogenicity, Taphonomy and Biodiversity. PLoS ONE, 2014, 9, e99438.	1.1	53
10	Organism motility in an oxygenated shallow-marine environment 2.1 billion years ago. Proceedings of the United States of America, 2019, 116, 3431-3436.	3.3	47
11	To be or not to be: postcubital vein in insects revealed by microtomography. Systematic Entomology, 2020, 45, 327-336.	1.7	47
12	Improved noninvasive microstructural analysis of fossil tissues by means of SR-microtomography. Applied Physics A: Materials Science and Processing, 2006, 83, 229-233.	1.1	42
13	In-situ interaction of cement paste and shotcrete with claystones in a deep disposal context. Numerische Mathematik, 2012, 312, 314-356.	0.7	42
14	Brief communication: Highâ€resolution assessment of the dental developmental pattern and characterization of tooth tissue proportions in the late Upper Paleolithic child from La Madeleine, France. American Journal of Physical Anthropology, 2009, 138, 493-498.	2.1	41
15	Vertebral microanatomy in squamates: structure, growth and ecological correlates. Journal of Anatomy, 2010, 217, 715-727.	0.9	38
16	Brief communication: Two human fossil deciduous molars from the sangiran dome (Java, Indonesia): Outer and inner morphology. American Journal of Physical Anthropology, 2012, 147, 472-481.	2.1	37
17	From outer to inner structural morphology in dental anthropology: integration of the third dimension in the visualization and quantitative analysis of fossil remains. , 2013, , 250-277.		29
18	Enamel thickness and enamel growth in Oreopithecus: Combining microtomographic and histological evidence. Comptes Rendus - Palevol, 2016, 15, 209-226.	0.1	26

#	Article	IF	CITATIONS
19	A Neanderthal from the Central Western Zagros, Iran. Structural reassessment of the Wezmeh 1 maxillary premolar. Journal of Human Evolution, 2019, 135, 102643.	1.3	25
20	The inner structural variation of the primate tibial plateau characterized by high-resolution microtomography. Implications for the reconstruction of fossil locomotor behaviours. Comptes Rendus - Palevol, 2010, 9, 349-359.	0.1	24
21	A Neanderthal partial femoral diaphysis from the "grotte de la Tourâ€, La Chaise-de-Vouthon (Charente,) Tj ET 581-593.	Qq1 1 0.78 0.1	84314 rgB⊤ 24
22	<i>Ouranopithecus macedoniensis</i> (Mammalia, Primates, Hominoidea): virtual reconstruction and 3D analysis of a juvenile mandibular dentition (RPI-82 and RPI-83). Geodiversitas, 2009, 31, 851-863.	0.2	21
23	Virtual dentitions: touching the hidden evidence. , 0, , 426-448.		20
24	Is the deciduous/permanent molar enamel thickness ratio a taxon-specific indicator in extant and extinct hominids?. Comptes Rendus - Palevol, 2017, 16, 702-714.	0.1	20
25	Collective behaviour in 480-million-year-old trilobite arthropods from Morocco. Scientific Reports, 2019, 9, 14941.	1.6	20
26	Development of a fracture network in crystalline rocks during weathering: Study of Bishop Creek chronosequence using X-ray computed tomography and ¹⁴ C-PMMA impregnation method. Bulletin of the Geological Society of America, 2016, 128, 1423-1438.	1.6	19
27	The earliest remains of a Citrus fruit from a western Mediterranean archaeological context? A microtomographic-based re-assessment. Comptes Rendus - Palevol, 2010, 9, 277-282.	0.1	18
28	Dental macrowear and cortical bone distribution of the Neanderthal mandible from Regourdou (Dordogne, Southwestern France). Journal of Human Evolution, 2019, 132, 174-188.	1.3	17
29	Calibration of digital autoradiograph technique for quantifying rock porosity using 14C-PMMA method. Journal of Radioanalytical and Nuclear Chemistry, 2015, 303, 11-23.	0.7	16
30	A crystallographic study of crystalline casts and pseudomorphs from the 3.5â€Ga Dresser Formation, Pilbara Craton (Australia). Journal of Applied Crystallography, 2018, 51, 1050-1058.	1.9	15
31	Structural analysis of premolar roots in Middle Pleistocene hominins from China. Journal of Human Evolution, 2019, 136, 102669.	1.3	13
32	X-ray microtomography applied to fossils preserved in compression: Palaeoscolescid worms from the Lower Ordovician Fezouata Shale. Palaeogeography, Palaeoclimatology, Palaeoecology, 2018, 508, 48-58.	1.0	12
33	Hominin diversity in East Asia during the Middle Pleistocene: AÂpremolar endostructural perspective. Journal of Human Evolution, 2020, 148, 102888.	1.3	11
34	Effective porosity measurements of poorly consolidated materials using non-destructive methods. Engineering Geology, 2016, 205, 24-29.	2.9	10
35	Mesoscale Anisotropy in Porous Media Made of Clay Minerals. A Numerical Study Constrained by Experimental Data. Materials, 2018, 11, 1972.	1.3	10

 $_{36}$ The role of volcanic-derived clays in the preservation of Ediacaran biota from the ItajaÃ-Basin (ca.) Tj ETQq0 0 0 rgBT $_{1.6}^{10}$ Overlock 10 Tf 50 $_{10}^{10}$

ARNAUD MAZURIER

#	Article	IF	CITATIONS
37	Digitization of Fossils from the Fezouata Biota (Lower Ordovician, Morocco): Evaluating Computed Tomography and Photogrammetry in Collection Enhancement. Geoheritage, 2019, 11, 1889-1901.	1.5	9
38	Frontoparietal Bone in Extinct Palaeobatrachidae (Anura): Its Variation and Taxonomic Value. Anatomical Record, 2015, 298, 1848-1863.	0.8	8
39	First evidence of Ediacaran-Fortunian elliptical body fossils in the Brioverian series of Brittany, NW France. Lethaia, 2018, 51, 513-522.	0.6	8
40	Using X-ray microtomography to characterize the burrowing behaviour of earthworms in heterogeneously polluted soils. Pedobiologia, 2020, 83, 150671.	0.5	8
41	The oldest human remains from the Beagle Channel region, Tierra del Fuego. International Journal of Osteoarchaeology, 2006, 16, 328-337.	0.6	7
42	Micro-computed tomographic and SEM study of porous bioceramics using an adaptive method based on the mathematical morphological operations. Heliyon, 2019, 5, e02557.	1.4	7
43	Growth and development of the third permanent molar in Paranthropus robustus from Swartkrans, South Africa. Scientific Reports, 2020, 10, 19053.	1.6	7
44	A morphometric mapping analysis of lower fourth deciduous premolar in hominoids: Implications for phylogenetic relationship between Nakalipithecus and Ouranopithecus. Comptes Rendus - Palevol, 2017, 16, 655-669.	0.1	4
45	Devonian agglutinated polychaete tubes: all in all it's just another grain in the wall. Proceedings of the Royal Society B: Biological Sciences, 2021, 288, 20211143.	1.2	2
46	The Neanderthal mandible BD 1 from La Chaise-de-Vouthon Abri Bourgeois-Delaunay (Charente,) Tj ETQq0 0 0 rg endostructural asymmetry. Paleo, 2020, , 346-359.	BT /Overlo 0.1	ck 10 Tf 50 2

47	Weathering of Viamão granodiorite, South Brazil: Part 1 – Clay minerals formation and increase in total porosity. Geoderma, 2022, 424, 115968.	2.3	2
48	Inner structural organization of the mandibular corpus in the late Early Pleistocene human	0.1	1

specimens Tighenif 1 and Tighenif 2. Comptes Rendus - Palevol, 2019, 18, 1073-1082. 48